A Re-examination of Spent Beam Refocusing for High-Efficiency Helix TWT's and Small MDC's

PETER RAMINS, SHELLY PEET, AND DALE A. FORCE, MEMBER, IEEE

Abstract—**The usefulness of the concept of spent beam refocusing in optimizing the performance of low- and medium-power helix TWT's equipped with small multistage depressed collectors (MDC's) is examined. Several direct comparisons of the performance of individually optimized TWT-MDC combinations with and without controlled beam expansion and recollimation are presented. The collector efficiency of a number of representative space and airborne TWT-MDC's, which do not use refocusing, is compared to a measure of quality (standard of excellence) established by an examination of irrecoverable MDC losses. The results suggest that the application of the traditional concept of spent beam refocusing to most helix TWT's that are equipped with small MDC's, in order to obtain maximum efficiency, is not required (or even desired). Two effects combine to obviate the need for refocusing: 1) the unexpanded beam more nearly meets the "point source" ideal at the input to the small MDC, and 2) the larger space-charge spreading and the slightly larger (but manageable) injection angles of the unexpanded beam can reduce the amount of backstreaming current and the attendant loss in efficiency.**

NOMENCLATURE

E_{r-sc}	Approximate (radial) space-charge field at the beam edge.
E_{z-col}	z-component of applied electric field near MDC input.
r_f	Radius of disk edge at output of refocuser.
r_i	Radius of disk edge at input to refocuser.
r_{col}	Maximum radius of active part of MDC.
r_{max}	Maximum disk edge radius (beam edge).
$S_n(\theta)$	Standard deviation of disk edge angles.
V_0	Cathode potential, with respect to ground.
J	Average current density in beam, based on r_{max}.
θ	Disk edge angle with respect to axis, $\tan^{-1}(V_r/V_z)$, where V_r and V_z are disk velocity components in cylindrical coordinate system.

I. INTRODUCTION

In EARLY studies of modern multistage collectors (MDC's) it was recognized that collector performance would be improved if the spent beam could be suitably conditioned prior to injection into the MDC [1]–[5]. These and other direct investigations of the refocusing of spent beams [6]–[8] led to the following generally accepted definition of the concept: a technique that combined 1) beam expansion to dilute space-charge density to the level where it is unimportant and 2) a reduction in the magnitude and range of radial velocity components of the spent beam prior to injection into the MDC. The concept of using the change (reduction) in the standard deviation of the electron (disk- or ring-edge in computer simulation) angles θ between the input and the output of the refocuser as one criterion for judging the effectiveness of the refocuser was introduced in [7] and used in subsequent spent beam refocusing investigations [9]–[12].

The benefits of spent beam refocusing were first demonstated in experiments with klystrons [13] and coupled cavity TWT's [14] (tubes that produce very broad distributions of electron energies and angles at the RF output), and MDC's sufficiently large to provide a good approximation to the "point source" ideal discussed by Kosmahl in [4] and [13]. Most of the subsequent applications of MDC technology (until recently) have involved low and medium power, space and airborne helix TWT's, and MDC's of very small size, with spent beam refocusing (as such) applied in only a limited number of cases (e.g., [15] and [16]). In most cases a short transition section (consisting of one or more full-strength permanent magnets in a continuation of the PPM stack) was used between the RF output and the MDC to make room for the output circuit assembly, or provide some spatial isolation between the RF output and any backstreaming current from the MDC.

In [17] and [18] it was demonstrated that the use of such a transistion section is compatible with the attainment of very high collector efficiency, even though drift through the transition resulted in increased beam disorder and (in some cases) beam compression rather than expansion. In these studies, the strengths of the individual permanent magnets of the transition section were considered as independent variables to experimentally optimize the MDC efficiency without any regard to the computed beam characteristics as such.

This paper examines the applicability (need) of the traditional concept of spent beam refocusing for applications requiring the highest possible overall efficiency, where low- or medium-power helix TWT's are to be used in conjunction with MDC's of very small size. It includes the following:

Manuscript received October 23, 1987.
P. Ramins and D. A. Force are with the NASA Lewis Research Center, Cleveland, OH 44135.
S. Peet was with the NASA Lewis Research Center, Cleveland, OH. She is now with Case Western University, Cleveland, OH 44106.
IEEE Log Number 8719366.

1) An examination of computed spent beam characteristics in conventional refocusers and in transition sections.

2) Analytically predicted and/or experimentally determined performance of MDC's individually optimized (for the same model TWT) for the case of beam expansion and re-collimation, as compared to drift in a transition region.

3) An example of collector performance as a function of size, for the case where (with beam expansion) beam diameter at the MDC input is no longer small compared to the MDC diameter.

4) An examination of the degree of success in achieving very high MDC efficiencies with a variety of TWT-MDC's that have only transition sections (no beam expansion) between the TWT and the MDC.

II. Analytical and Experimental Procedures and Techniques

An analytical and experimental program was conducted to obtain direct comparisons of MDC performance for cases where the same basic model TWT was operated in conjunction with the two types of spent beam refocusing systems discussed above: 1) beam expansion and re-collimation, and 2) drift in a transition section. For convenience, these will be labeled "with expansion" and "without expansion" in the following sections of this report. The MDC designs were individually optimized using the verified TWT-Refocuser-MDC design procedure described in [15] and [17]. In other cases, the collector efficiencies achieved either in design or actual operation by TWT-Transition Section-MDC combinations were evaluated in order to put some limits on the improvement in performance (if any) possible with an optimized refocusing system in place of the transition section.

Extensive use was made of published results, as well as completed (but unpublished) TWT-MDC design exercises. This ready availability of certain pertinent results led to the particular choices of TWT-MDC designs for evaluation and comparison. The iterative computational design procedure does not guarantee optimum results; however, considerable effort had gone into optimizing most of the MDC designs.

The experimental techniques described in [11] were used, in some cases, to optimize and measure MDC efficiencies. In other tests with small TWT-MDC vacuum envelopes, where the TWT body losses (sum of circuit losses and beam interception losses in the forward direction) had not been measured directly, some assumptions were required to obtain MDC efficiencies [19], [20]. In some cases these were based on measured body losses in very similar TWT's. In other cases, where the body losses were estimated, the rationale and specific values can generally be found in the appropriate references given. In all of the cases where assumptions were used, the collector efficiencies were labeled as "estimated."

The considerations and technique outlined by Kosmahl in [21] can be used to estimate the overall TWT and MDC efficiencies of various helix TWT-MDC combinations, for given values of electronic efficiency, perveance, and number of MDC stages. The values of MDC efficiency calculated from the formulas given in [21] are close to the upper limit obtainable for any specific TWT-MDC since they are based on an analysis of fundamental (irrecoverable) MDC losses: 1) those associated with radial velocity components (sorting), 2) those associated with a finite number of MDC stages used to collect a beam with a range of electron energies (as determined by the TWT electronic efficiency and perveance), and 3) the presence of electrons having significantly more energy than eV_0. Any favorable grouping of electrons in the spent beams of actual TWT's into velocity classes (as opposed to the triangular distribution assumed in [21]) creates the potential for enchanced MDC efficiency. The magnitude of this improvement decreases with the number of collector stages. However, this approximate technique for computing collector efficiency neglects secondary electron emission losses in the MDC, and these can be of sufficient magnitude to largely offset the potential enhancement of collector efficiency due to favorable grouping.

This technique was used to establish what would constitute excellent collector efficiency for each of a number of specific TWT designs. The calculations assumed a collector sorting efficiency of 97 percent and a 1-percent fixed loss associated with the fast electrons [21]. In most cases the normalized value of the kinetic energy of the slowest electron at the MDC input ($E_{\min}$ in [21]) was determined from the Helical TWT Computer Program [15] and not the approximate technique given in [21] for conventional (non-dynamic velocity taper) helix TWT's. The difference between this "approximate upper limit" on collector efficiency and the measured and/or computed values for optimized designs (with transition section) was used to determine whether the use of refocusing might have yielded significantly better results.

III. TWT-Refocuser-MDC Performance With and Without Beam Expansion

A. Teledyne MEC Dual-Mode TWT

The general characterisitics of the TWT are shown in Table I. Model MTZ-7000 is a broad-band medium-power medium-perveance TWT. The charge trajectories are shown in Figs. 1 and 2 for the low and high modes, respectively. The spent beam characteristics at the input to and the output of the refocusing section are summarized in Tables II and III. It is evident that the case with expansion meets the generally accepted criteria for good spent beam refocusing: 1) controlled expansion to the point where current density is low, and 2) a simultaneous improvement in laminarity (as evidenced by the substantial reductions in the standard deviation of disk edge angles and the number of disk edge angles that are negative). For the case of drift through a transition section, however, the net effect appears to be unfavorable: no expansion (based on the average radius) and increases in both the standard deviation of θ and in the number of negative angles. The

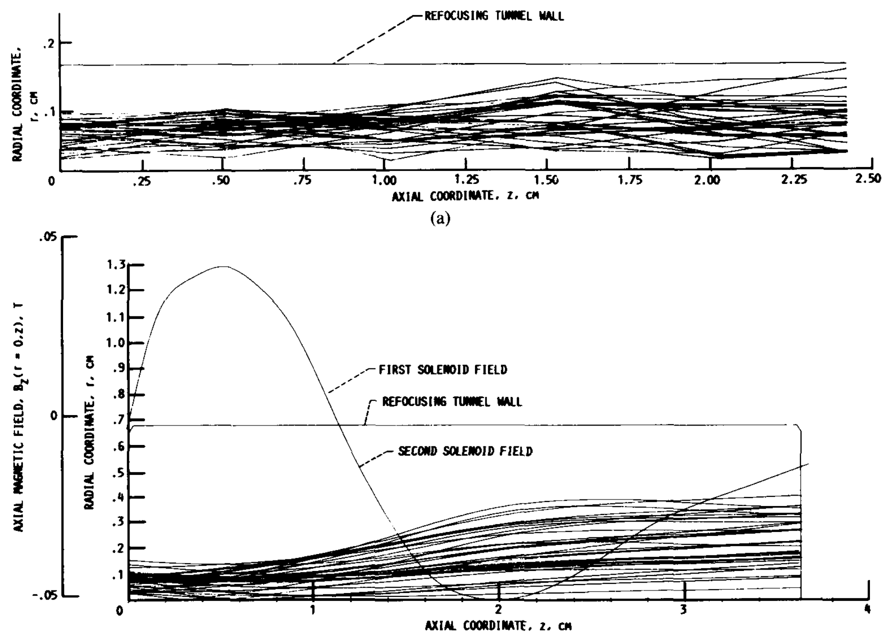

Fig. 1. Charge trajectories and refocusing field profile in refocusing section for TWT operation at saturation in low mode. Optimized for low mode. (a) Without and (b) with beam expansion.

TABLE I
GENERAL CHARACTERISTICS OF T MEC DUAL-MODE TWT MODEL MTZ-7000

Mode	Frequency, GHz	Nominal RF output power, W	Typical electronic efficiency, percent	Perveance, $A/V^{3/2} \times 10^{-6}$
Low	4.8 to 9.6	500	15.5	0.4
High		750	19.0	.5

TABLE II
PERFORMANCE OF SPENT BEAM REFOCUSERS FOR TELEDYNE MEC DUAL-MODE TWT MODEL MTZ-7000

(a) Low mode

Type of refocuser	Average disk edge radius, mm		$(r_f/r_i)_{edge}$	Area expansion for beam edge	Average angle of disk edge, deg		Standard deviation of angle, deg		Fraction of negative angles	
	Initial	Final			Initial	Final	Initial	Final	Initial	Final
With expansion	0.73	2.4	2.6	6.8	-1.2	1.6	3.2	1.3	22/32	3/32
Without expansion	.60	.73	1.6	2.7	.1	-1.2	2.4	3.2	15/32	22/32

(b) High mode

Type of refocuser	Average disk edge radius, mm		$(r_f/r_i)_{edge}$	Area expansion for beam edge	Average angle of disk edge, deg		Standard deviation of angle, deg		Fraction of negative angles	
	Initial	Final			Initial	Final	Initial	Final	Initial	Final
With expansion	0.65	2.7	3.4	12	-0.8	0.6	3.8	2.2	17/32	9/32
Without expansion	.67	.65	1.3	1.6	.6	-0.8	3.4	3.8	16/32	17/32

average current density of the unexpanded beams, of 5 to 10 A/cm^2, is considerably higher than the goal of less than 1 A/cm^2 in early experiments with large collectors [4]. The quantity $E_{z-\mathrm{col}}/E_{r-sc}$ shown in Table III is a measure of the importance of space charge in the collector. It was computed for the edge of the beam using the assumption of uniform current density in the beam and a typical value of E_z near the MDC entrance, and is only

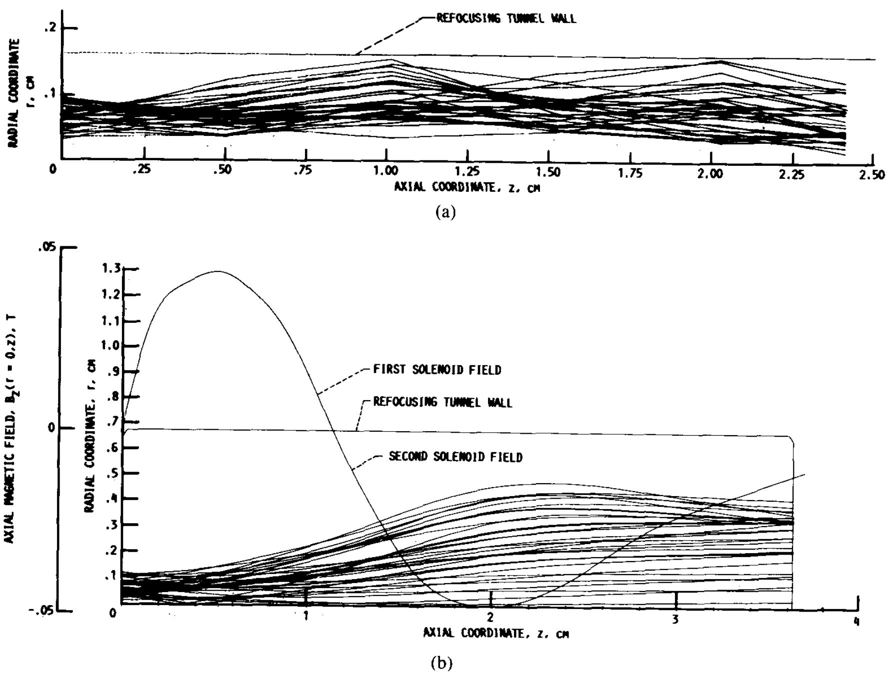

Fig. 2. Charge trajectories and refocusing profile in refocusing section for TWT operation at saturation in high mode. Optimized for low mode. (a) Without and (b) with beam expansion.

TABLE III
SPENT BEAM CHARACTERISTICS OF T MEC DUAL-MODE TWT MODEL MTZ-7000 AT INPUT TO 2.4-cm-DIAMETER MDC

(a) Low mode				
Type of refocuser	r_{col}/r_{max}	Beam current density, A/cm^2	Minimum $E_{z\text{-}col}/E_{r\text{-}sc}$	Maximum positive/negative angle of disk centroid, deg
With expansion	3.0	0.8	9	3.4/-1.2
Without expansion	7.8	5	9	3.5/-4.4

(b) High mode				
Type of refocuser	r_{col}/r_{max}	Beam current density, A/cm^2	Minimum $E_{z\text{-}col}/E_{r\text{-}sc}$	Maximum positive/negative angle of disk centroid, deg
With expansion	2.9	0.9	7	3.1/-3.8
Without	9.8	10	6	3.9/-5.8

approximate. The values for the expanded and the unexpanded beams are comparable because of the considerably stronger E_z in the MDC design optimized for the unexpanded beam. A comparison of the electric field distribution in the collector, with and without the unexpanded beam, showed some significant differences, indicating that space-charge effects are significant in determining electron trajectories in the MDC. The space charge measurably increases beam dispersion (outward radial deflection), overcoming (in some regions of the MDC) potentially dangerous convergent lens effects. For the expanded beam, the space-charge effects in the MDC were smaller but still quite noticeable. The range of angles is significantly wider for the unexpanded beams, but their sizes at the input to the MDC are smaller fractions of the MDC size.

The geometries of the 2.4-cm-diameter 4-stage collectors, individually optimized for the two input beams, are shown in Fig. 3, along with the charge trajectories for the low mode. The computed TWT-MDC performance is summarized in Table IV. The measured TWT-MDC performance is summarized in Table V [22], [23]. Both the computed and the measured efficiency of the two MDC's are almost identical. This was true for both the computed and measured MDC efficiencies for the high mode as well. The performance of the MDC with the unexpanded beam is actually somewhat superior because 1) with equivalent electrode surface secondary electron emission characteristics (carbon black) its efficiency would be significantly higher, and 2) because the experimental TWT in this case exhibited a higher RF efficiency and, therefore, a slightly lower collector efficiency would be expected [21]. The length of the collector (axial extent from the output polepiece) is somewhat smaller for the unexpanded beam because of the stronger space-charge effects (spreading) and the slightly larger injection angles, and its sorting efficiency is slightly lower (larger radial velocities). However, it produces less backstreaming current to ground potential. For expanded beams injected into small MDC's, a significant loss in efficiency can be caused by the inability of the collector to handle low-energy electrons that are near the edge of the beam and have small negative angles. These tend to backstream to the TWT body and

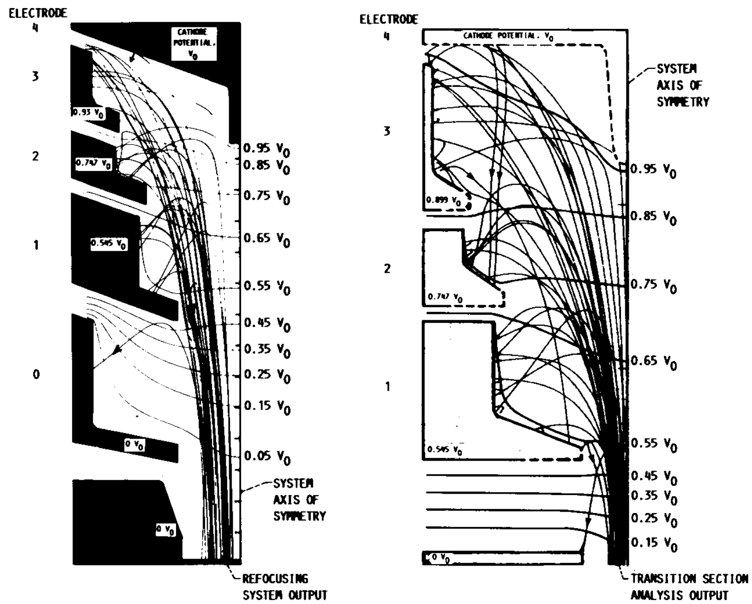

Fig. 3. Charge trajectories in four-stage 2.4-cm-diameter depressed collectors. T MEC dual-mode TWT operating at saturation in low mode. (a) With and (b) without beam expansion.

TABLE IV
ANALYTICAL PERFORMANCE OF T MEC DUAL-MODE TWT AND 2.4-cm-DIAMETER FOUR-STAGE COLLECTOR, WITH AND WITHOUT BEAM EXPANSION
(TWT operating at saturation at 8.4 GHz in low mode.)

Type of refocuser	RF efficiency, percent	Overall efficiency, percent	Collector efficiency,[1] percent
With expansion	13.5	45.8	83.3
Without expansion	13.5	46.1	83.4

[1]Secondary electron yield, $\delta = 0.6$.

TABLE V
EXPERIMENTAL PERFORMANCE OF T MEC DUAL-MODE TWT AND 2.4-cm-DIAMETER FOUR-STAGE COLLECTORS, WITH AND WITHOUT BEAM EXPANSION
(TWT operating at saturation in low mode.)

(a) At 8.4 GHz

Refocuser characteristics and TWT model	MDC electrode surface	RF efficiency, percent	Overall efficiency, percent	Collector efficiency, percent
With beam expansion (TWT Model MTZ-7000)	Carbon black	13.6	43.9	83.3
Without beam expansion (TWT Model MTH-5065)[1]	Machined isotropic graphite	16.8	49.7	83.1[2]

(b) Average performance, 4.8 to 9.6 GHz

Refocuser characteristics and TWT model	MDC electrode surface	RF efficiency, percent	Overall efficiency, percent	Collector efficiency, percent
With beam expansion (TWT Model MTZ-7000)	Carbon black	12.5	41.1	82.8
Without beam expansion (TWT Model MTH-5065)[1]	Machined isotropic graphite	14.1	44.3	82.7[2]

[1]A TWT of almost identical design to MTZ-7000.
[2]Estimated value. TWT body power based on measured values for MTZ-7000.

TABLE VI
EXPERIMENTAL PERFORMANCE OF T MEC MODEL MTZ-7000 TWT WITH BEAM EXPANSION AND A 5.0-cm-DIAMETER FOUR-STAGE COLLECTOR
(Average performance at saturation, 4.8 to 9.6 GHz in low mode.)

Type of refocuser and TWT model	r_{col}/r_{max}	Overall efficiency, percent	Collector efficiency, percent
With beam expansion (TWT Model MTZ-7000)	6.3	43.7	85.1

TABLE VII
GENERAL CHARACTERISTICS OF VARIAN TWT MODEL 6336 A1

Frequency, GHz	RF output power, W	Electronic efficiency, percent	Perveance, $A/V^{3/2}(\times 10^{-6})$
2.5 to 5.5	750	27.3	1.15

TABLE VIII
PERFORMANCE OF SPENT BEAM REFOCUSERS FOR VARIAN HIGH-PERVEANCE TWT MODEL 6336 A1

Type of refocuser	Average disk edge radius, mm		$(r_f/r_i)_{edge}$	Area expansion for beam edge	Average angle of disk edge, deg		Standard deviation of angle, deg		Fraction of negative angles	
	Initial	Final			Initial	Final	Initial	Final	Initial	Final
With expansion	1.1	3.5	3.2	10.0	0.5	0.9	5.6	4.2	16/32	9/32
Without expansion	1.4	1.1	.9	.8	.5	.5	4.1	5.6	13/32	16/32

TABLE IX
SPENT BEAM CHARACTERISTICS OF VARIAN TWT MODEL 6336 A1 AT INPUT TO 2.4-cm-DIAMETER MDC

Type of refocuser	r_{col}/r_{max}	Beam current density, A/cm^2	Minimum E_{z-col}/E_{r-sc}	Maximum positive/negative angle of disk centroid, deg
With expansion	2.1	0.5	13	4.9/-6.7
Without expansion	6.7	5	10	10.7/-7.0

produce a significant reduction in efficiency. This is particularly true for the widely used "individual-lens" type collectors ("ILC," discussed by Kosmahl in [13]) which do not automatically provide outward radial deflection forces throughout the collector. This problem with small negative angles near the beam edge is particularly acute for MDC's that deviate significantly from the "point source" ideal. The ratios of collector to input beam edge diameters are shown in Table III. It is evident that the expanded input beams deviate greatly from the "point source" ideal. Consequently, *low input beam current density and good laminarity (as measured by $S_n(\theta)$), do not, of themselves, appear to be adequate criteria for selecting suitable refocuser designs for various MDC applications.*

The measured performance of a larger MDC operated in conjunction with the same TWT and expanded beam is shown in Table VI. Comparison of these results to those in Table V(b) shows that, when a reasonably good value of r_{col}/r_{max} is achieved, the higher sorting efficiency achieved with the expanded beam will yield higher collector efficiencies.

B. Varian High-Perveance TWT

The general characteristics of the TWT are shown in Table VII. Varian model 6336 A1 is a broad-band high-electronic-efficiency TWT. The spent beam characteristics at the input to and the output of the refocusing section are shown in Table VIII. As was the case with the TWT discussed in the preceding section of this report, the refocuser with beam expansion provides controlled expansion to dilute beam current density to less than 1 A/cm^2 and improve beam laminarity. Drift in the transition section produced the opposite results. However, as can be seen from Table IX, the unexpanded beam yields a much better approximation to the "point source" ideal at the MDC input; and, even with the high perveance of the TWT, space-charge effects are not dominant. The extreme angles are fairly large but manageable.

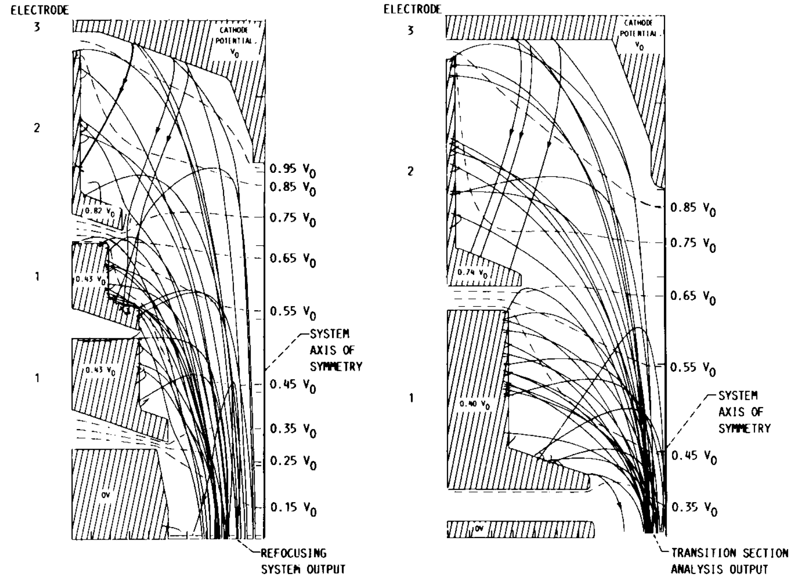

(a) (b)

Fig. 4. Charge trajectories in three-stage 2.4-cm-diameter depressed collectors. VA TWT operating at saturation at 4.75 GHz. (a) With and (b) without beam expansion.

TABLE X
ANALYTICAL PERFORMANCE OF VARIAN TWT MODEL 6336 A1 AND 2.4-cm-DIAMETER THREE-STAGE COLLECTOR, WITH AND WITHOUT BEAM EXPANSION
(TWT operating at saturation at 4.75 GHz.)

Type of refocuser	RF efficiency, percent	Overall efficiency, percent	Collector efficiency,[1] percent
With expansion	25.5	55.5	74.0[2]
Without expansion	25.5	56.3	75.1

[1]Secondary electron yield, δ = 0.6.
[2]For intermediate MDC design (Ref. 16).

The geometries of the two 2.4-cm-diameter three-stage collectors, and the charge trajectories are shown in Fig. 4. The computed TWT-MDC performance is summarized in Table X. The MDC design for the expanded beam is one of the intermediate designs generated in an optimization study [16] and is near but not necessarily fully optimized. This study consistantly showed computed collector efficiencies about one half a percent higher than experimentally optimized measured efficiencies. This would suggest an optimized analytical three-stage collector efficiency slightly in excess of the measured value of 75.5 percent for the final (optimized) design [24]. This value is very close to the optimized computed result with no beam expansion.

IV. Performance of TWT-MDC'S Without Beam Expansion

The rationale for using the magnitude of MDC efficiency, as calculated from the formulas given in [21] as a measure of what constitutes excellent MDC performance for any conventional helical TWT was discussed earlier. For convenience, these calculated values will be referred to as "expected collector efficiency."

The analytical and experimental performance of some representative space and airborne TWT-MDC designs are compared to the "expected collector efficiency" in Table XI. Each of these TWT's has a transition section, consisting of the continuation of the full-strength PPM stack for $1\frac{1}{4}$ or more periods, between the RF output and the MDC. All of the MDC's are of the axisymmetric type with an on-axis spike at cathode potential. The table lists the tube parameters that affect collector efficiency. It is evident that the analytical and experimental MDC efficiencies closely approach the expected efficiencies. In two of the analytical cases the computed collector efficiencies exceed the expected value. In the case of all of the experimental collectors, the use of electrode surfaces with reduced secondary electron emission characteristics (e.g., textured carbon) would significantly improve the collector efficiencies and, based on [25], bring them very close to (or in excess of) the expected values.

Consequently, it appears that it is possible to design highly efficient small MDC's for low-and medium-power helix TWT's that use only transition sections between the TWT output and MDC. Little (if any) improvement in the overall TWT and collector efficiencies would be expected if the transition sections were replaced by refocusers, which provide beam expansion and re-collimation.

The spent beam characteristics at the beginning and end of the transition section for three of these TWT's are shown in Table XII. In all cases, beam compression rather than expansion takes place, and $S_n(\theta)$ increases. In two

TABLE XI

COMPARISON OF COMPUTED OR MEASURED COLLECTOR EFFICIENCIES OF VARIOUS SPACE AND AIRBORNE TYPE TWT-REFOCUSER-MDC'S WITH NO BEAM EXPANSION TO THE EXPECTED PERFORMANCE OF A HIGHLY OPTIMIZED MDC DESIGN (SEE TEXT)

(a) Analytical results

TWT-MDC characteristics	Perveance $A/V^{3/2}$ ($\times 10^{-6}$)	Electronic efficiency, percent	Analytical collector efficiency,[1] percent	Expected collector efficiency,[2] percent	Reference
275 W, 8-18 GHz 4 stage	0.284	16.2	85.4	86.9	17
20 W, 12 GHz 3 stage	.144	19.6	81.1	81.3	[ ][3]
50 W, 12 GHz 4 stage	.122	18.3	89.2	87.5	[ ][3]
75 W, 20 GHz 5 stage	.065	12.0	91.1	92.7	[ ][3]
20 W, 8.4 GHz 4 stage	.16	27.8	87.7	86.9	29

(b) Experimental results

TWT-MDC characteristics		Frequency, GHz	Perveance $A/V^{3/2}$ ($\times 10^{-6}$)	Electronic efficiency, percent	MDC electrode surface charac-teristic	Estimated collector efficiency, percent	Expected collector efficiency, percent	Reference
275 W, 8-18 GHz 4 stage		13	0.26	16.4	Machined isotropic graphite	86.2	86.9	17
HAC multi-mode 5 stage 5-cm	Saturation Low mode	19	0.023	4.9	Titanium carbide	92.5	93.5	26
	5 dB below saturation	19	0.023	1.8	TiC	94.0	94.6	26
HAC 918H, 55 W 20 GHz		19.2	0.044	12	TiC	90.7	93.1	27
T MEC MTH 5065 4.8-9.6 GHz, 550 W		8.4	0.40	19.5	Machined isotropic graphite	83.2	84.5	18

[1]Computed by the design technique described in Ref. 17 for a specific MDC geometry and electrode material.
[2]Calculated value from considerations outlined in Ref. 21, used as an estimate of what constitutes a very high collector efficiency for a given TWT.
[3]NASA design study (unpublished).

TABLE XII

SPENT BEAM CHARACTERISTICS BEFORE AND AFTER DRIFT IN CONTINUATION OF FULL-STRENGTH PPM STACK (TRANSITION SECTION) FOR VARIOUS TWT'S

TWT characteristics	Average disk edge radius, mm		$(r_f/r_i)_{edge}$	Area expansion for beam edge	Average angle of disk edge, deg		Standard deviation of angle, deg		Fraction of negative angles	
	Initial	Final			Initial	Final	Initial	Final	Initial	Final
275 W, 8-18 GHz	0.35	0.28	0.8	0.6	0.9	0.2	2.6	3.3	11/32	15/32
50 W, 12.2 GHz	.29	.22	.8	.6	-2.7	-1.6	2.1	2.6	30/32	24/32
20 W, 12.2 GHz	.19	.17	.8	.6	1.0	-.4	1.8	2.6	9/32	16/32

of the transition sections the number of negative angles increases as well. The increase in $S_n(\theta)$ in these and the other transition sections discussed earlier is in agreement with the observed growth in the disorder (up to a point) in beams in drifting through PPM stacks [28]. The rather chaotic charge trajectories in the transition section of the 275-W, 8- to 18-GHz TWT are shown in [17, Fig. 3]. However, as can be seen from Table XIII, 1) a very favorable collector to beam diameter ratio is achieved, 2) the injection angles are manageable, and 3) space-charge effects in the small-sized MDC's are not dominant even with the relatively high injection current densities of 10 to 20 A/cm^2.

TABLE XIII

UNEXPANDED SPENT BEAM CHARACTERISTICS FOR VARIOUS TWT'S AT INPUT TO SMALL-SIZED MDC

TWT-MDC characteristics	r_{col}/r_{max}	Beam current density, A/cm^2	Minimum, E_{z-col}/E_{r-sc}	Maximum positive/negative angle of disk centroid, deg
275 W, 8-18 GHz TWT and 1.7-cm diameter MDC	13.5	22	8	5.4/-5.2
50 W, 12.2 GHz TWT and 2.0-cm diameter MDC	28	8	15	2.2/-5.4
20 W, 12.2 GHz TWT and 2.0-cm diameter MDC	34	12	10	3.1/-5.2

V. Concluding Remarks

The usefulness of the concept of spent beam refocusing for maximizing the efficiency of low-and medium-power space and airborne TWT's equipped with small MDC's was examined. A distinction was made between refocusers that provide controlled beam expansion and recollimation and simple transition sections between the TWT and MDC that serve merely to confine the spent beam until it can be injected into the MDC or isolate the TWT from the MDC. Several direct comparisons of TWT-MDC performance with and without optimized spent beam refocusing were presented. The computed or measured performance of a number of representative space and airborne TWT-MDC's, which use transition sections rather than optimized refocusers, was compared to an approximate upper limit on the collector efficiency, as established by an examination of the irrecoverable collector losses for that particular TWT application. These comparisons suggest that the application of spent beam refocusing to most helix TWT's equipped with small MDC's is not required in order to maximize TWT-MDC efficiency. Several effects combine to obviate the need for optimized refocusing:

1) The size of some expanded beams at the input to the MDC becomes a substantial fraction of the collector diameter, deviating greatly from the "point source" ideal.

2) The stronger electric fields in small-size MDC's permit the injection of higher current density beams (compared to the 1-A/cm^2 values typical in early large-size MDC's) without excessive space-charge spreading and consequent reduction in the sorting efficiency.

3) The larger angles and space-charge spreading of the unexpanded beams reduces the amount of backstreaming current to the TWT body and the attendant loss in efficiency.

4) The basic MDC design (axisymmetric, with an axial spike at cathode potential) can readily accommodate the reasonably narrow range of injection angles typically generated by helical TWT's (as opposed to, e.g., high-efficiency klystrons and coupled-cavity TWT's).

This investigation was limited to TWT's that operate at saturation in conjunction with small MDC's and the conclusions reached apply only to such applications. For applications that require maximum efficiency for operation of TWT's in the linear range (typically four or more decibels below saturation), it is quite possible that optimally expanded beams would yield better results. For the resulting narrowed range of electron energies, expanded beams with very favorable characteristics (small positive angles; see, e.g., [15, Figs. 5, 6, and 10]) can be obtained. For such beams the "point source" ideal is not as important as the highest possible sorting efficiency in the MDC.

In the case of high-power helix TWT's and (in some cases) the possible use of larger MDC's, the need for optimized beam expansion remains to be evaluated.

References

[1] O. G. Sauseng, A. Basiulis, and I. Tammaru, "Analytical study program to develop the theoretical design of traveling-wave tubes," NASA CR-72450, 1968.

[2] T. G. Mihran and W. Neugebauer, "Analytic study of a depressed collector for linear beam microwave amplifiers," NASA CR-72768, July 8, 1970.

[3] W. Neugebauer and T. G. Mihran, "Multistage depressed electrostatic collector for magnetically focused space borne klystrons," NASA CR-72767, 1970.

[4] H. G. Kosmahl, "A novel, axisymmetric electrostatic collector for linear beam microwave tubes," NASA TN D-6093, 1971.

[5] I. Tammaru, "Multistage depressed collector investigation for traveling-wave tubes," NASA CR-72950, 1971.

[6] ——"Refocusing of the spent axisymmetric beam in coupled cavity traveling wave tubes," NASA CR-120893, 1971.

[7] G. M. Branch and W. Neugebauer, "Refocusing of the spent axisymmetric beam in klystron tubes," NASA CR-121114, 1972.

[8] H. G. Kosmahl, "An electron beam controller," U.S. Patent 3 764 850, Oct. 1973.

[9] N. Stankiewicz, "Evaluation of magnetic refocusing in linear-beam microwave tubes," NASA TN D-7660, 1974.

[10] ——"Analysis of spent beam refocusing to acheive optimun collector efficiency," *IEEE Trans. Electron Devices*, vol. ED-24, pp. 32–36, 1977.

[11] H. G. Kosmahl and P. Ramins, "Small-size 81- to 83.5-percent efficient 2- and 4-stage depressed collectors for octave-bandwidth high-performance TWT's," *IEEE Trans. Electron Devices*, vol. ED-24, pp. 36–44, 1977.

[12] K. H. Krause, "A dynamic refocusing system for linear beam microwave tubes," Engineering degree thesis, Stanford Univ., Stanford, CA, 1979.

[13] H. G. Kosmahl, "Modern multistage depressed collectors—A review," *Proc. IEEE*, vol. 70, pp. 1325–1334, 1982.

[14] C. L. Jones, "A 200 Watt traveling wave tube for the communications technology satellite," NASA CR-135029, 1976.

[15] J. A. Dayton, Jr., G. Kosmahl, P. Ramins, and N. Stankiewicz, "Experimental verification of computational procedure for the design of TWT-refocuser-MDC systems," *IEEE Trans. Electron Devices*, vol. ED-28, pp. 1480–1489, 1981.

[16] J. A. Dayton, Jr., H. G. Kosmahl, and P. Ramins, "Experimental verification of the multistage depressed collector design procedure for a high-perveance, helix-type, traveling-wave tube," NASA TP-2162, 1983.

[17] P. Ramins, H. G. Kosmahl, D. A. Force, R. W. Palmer, and J. A. Dayton, "Verification of an improved computational design procedure for TWT-dynamic refocuser-MDC systems with secondary electron emission losses," *IEEE Trans. Electron Devices*, vol. ED-33, pp. 85–90, 1986.

[18] P. Ramins, D. A. Force, and H. G. Kosmal, "Analytical and experimental performance of a dual-mode traveling-wave tube and multistage depressed collector," NASA TP-2752, 1987.

[19] H. G. Kosmahl, "Comments on measuring the overall and the depressed collector efficiency in TWT's and klystron amplifiers," *IEEE Trans. Electron Devices*, vol. ED-26, p. 156, 1979.

[20] A. S. Gilmour, Jr., *Microwave Tubes*. Norwood, MA: Artech, 1986.

[21] H. G. Kosmahl, "How to quickly predict the overall TWT and the multistage depressed collector efficiency," *IEEE Trans. Electron Devices*, vol. ED-27, pp. 526–529, 1980.

[22] P. Ramins and T. A. Fox, "Performance of computer-designed small-sized four-stage depressed collector for operation of dual-mode traveling wave tube," NASA TP-1832, 1981.

[23] P. Ramins *et al.*, "Performance of a small graphite electrode, multistage depressed collector with a 500-W, CW, 4.8 to 9.6 GHz traveling wave tube," NASA TP-2788, 1988.

[24] P. Ramins, "Performance of computer-designed small-size multistage depressed collectors for a high-performance traveling wave tube," NASA TP-2248, 1984.

[25] P. Ramins and B. T. Ebihara, "Improvements in MDC and TWT overall efficiency through the application of carbon electrode surfaces," *IEEE Trans. Electron Devices*, vol. ED-33, pp. 1915–1924, 1986.

[26] R. N. Tamashiro, "20 GHz, 75 Watt helix traveling wave tube for space communications," NASA CR-168271, 1984.

[27] M. McDermott and R. Tamashiro, "20 GHz, 50 Watt helix traveling wave tube," NASA CR-174881, 1985.

[28] R. True, "Emittance and the design of beam formation, transport, and collection systems in periodically focussed TWT's," *IEEE Trans. Electron Devices*, vol. ED-34, pp. 473–485, 1987.

[29] A. N. Curren *et al.*, "High efficiency helical TWT with dynamic velocity taper and advanced multistage depressed collector, presented at the Int. Electron Devices Meeting, Washington, DC, Dec. 7–9, 1987.

Peter Ramins, photograph and biography not available at the time of publication.

*

Shelly Peet, photograph and biography not available at the time of publication.

*

Dale A. Force (M'84), photograph and biography not available at the time of publication.